

Abstract

The natural abundance of ^{14}C in total CO_2 dissolved in seawater is a property applied to evaluate the water age structure and circulation in the ocean and in ocean models. In this study we use three different representations of the global ocean circulation augmented with a suite of idealised tracers to study the potential and limitations of using natural ^{14}C to determine water age, the time elapsed since a body of water had contact with the atmosphere. We find that, globally, bulk ^{14}C -age is dominated by two equally important components, one associated with aging, i.e. the time component of circulation and one associated with a “preformed ^{14}C -age”. This latter quantity exists because of the slow and incomplete atmosphere/ocean equilibration of ^{14}C in particular in high latitudes where many water masses form. The relative contribution of the preformed component to bulk ^{14}C -age varies regionally within a given model, but also between models. Regional variability, e.g. in the Atlantic Ocean is associated with the mixing of waters with very different end members of preformed ^{14}C -age. In the Atlantic, variations in the preformed component over space and time mask the circulation component to an extent that its patterns are not detectable from bulk ^{14}C -age alone. Between models the variability of age can also be considerable (factor of 2), related to the combinations of physical model parameters, which influence circulation dynamics, and gas exchange in the models. The preformed component was found to be very sensitive to gas exchange and moderately sensitive to ice cover. In our model evaluation exercise, the choice of the gas exchange constant from within the current range of uncertainty had such a strong influence on preformed and bulk ^{14}C -age that if model evaluation would be based on bulk ^{14}C -age it could easily impair the evaluation and tuning of a models circulation on global and regional scales. Based on the results of this study, we propose that considering preformed ^{14}C -age is critical for a correct assessment of circulation in ocean models.

^{14}C -age tracers in global ocean circulation models

W. Koeve et al.

Title Page

Abstract

Introduction

Conclusions

References

Tables

Figures



Back

Close

Full Screen / Esc

Printer-friendly Version

Interactive Discussion



1 Introduction

Coupled global ocean circulation models are the method of choice for studying the role of the oceans under a changing climate. They are, for example, used to predict future changes of biogeochemical cycles in the ocean. In the context of ocean biogeochemistry the time elapsed since the last contact of a water parcel with the atmosphere is of particular interest in order to understand the interaction of changes in climate, circulation and biogeochemical processes. A variety of tracers can be used to evaluate circulation and water age structure both in the real ocean and in biogeochemical ocean models (e.g. Lynch-Stieglitz, 2003). One tracer, ^{14}C -DIC, has become pivotal in such studies (Stuiver et al., 1983; Toggweiler et al., 1989; Jain et al., 1995; Caldeira et al., 2002; Matsumoto et al., 2004; Cao and Jain, 2005; Matsumoto, 2007). ^{14}C is naturally produced in the upper atmosphere to reach rather constant atmospheric levels and enters the ocean via gas exchange. In the ocean's interior, there is no ^{14}C production, and radioactive decay with a half-life of 5730 yr reduces its concentration over time. This leads to a decrease of the $^{14}\text{C}/\text{C}$ ratio of dissolved inorganic carbon, which allows the computation of ^{14}C -ages (yr) of the respective water (for equations see Sect. 2). The natural distribution of ^{14}C in the ocean is often expressed in a delta notation relative to the $^{14}\text{C}/\text{C}$ ratio of the atmosphere ($\Delta^{14}\text{C} = (R_o/R_a - 1) \cdot 1000$; R_o , R_a are the $^{14}\text{C}/\text{C}$ ratios of ocean and atmosphere (1890 AD, Stuiver and Polach, 1977), respectively). Surface water in equilibrium with the preindustrial atmosphere (1890 AD) would have a $\Delta^{14}\text{C} = 0\text{‰}$ and a ^{14}C -age of 0 yr.

Several issues complicate the use of natural ^{14}C for data-based evaluation of ocean-model circulation. First, there is the assumption of constant atmospheric ^{14}C -boundary conditions often applied in ocean model ^{14}C -experiments. On multi-millennial time scales, the atmospheric ^{14}C -production and level is by no means constant (Bard, 1988; Adkins and Boyle, 1997; Franke et al., 2008a, b). Secondly, there are significant man-made changes to the $^{14}\text{C}/\text{C}$ distribution in the atmosphere and the ocean. The invasion of fossil fuel CO_2 , almost devoid of ^{14}C , into the ocean reduces the $^{14}\text{C}/\text{C}$

GMDD

7, 7033–7074, 2014

^{14}C -age tracers in global ocean circulation models

W. Koeve et al.

Title Page

Abstract

Introduction

Conclusions

References

Tables

Figures



Back

Close

Full Screen / Esc

Printer-friendly Version

Interactive Discussion



ratio (the Suess Effect; Suess, 1955). On the other hand, ^{14}C - CO_2 from atmospheric nuclear-bomb testing in the 1960s has strongly increased it (Rafter and Fergusson, 1957). The combination of both effects masks the natural distribution of $^{14}\text{C}/\text{C}$ in the ocean considerably, in particular in the upper ocean (e.g. Stuiver, 1980 and Fig. 1a).
5 Thirdly, it is usually assumed that the transport of $^{14}\text{C}/\text{C}$ from the surface to the deep sea via sinking organic particles can be neglected (Fiadeiro, 1982).

Finally, the time to reach equilibration of atmosphere and surface ocean for ^{14}C - CO_2 is in the order of a decade (Broecker and Peng, 1974), which is longer than water residence at the surface. In particular, the entrainment of old, ^{14}C -depleted water does not
10 allow surface $^{14}\text{C}/\text{C}$ ratios to reach equilibrium with the atmosphere. Thus ^{14}C -ages in the surface ocean (after bomb- ^{14}C correction) are on the order of hundreds of years (Fig. 1b). Elevated surface ages have been confirmed by radiocarbon measurements in warm-water corals from times before bomb testing or before the industrial era (e.g. Druffel, 1981) indicating that they are not an artefact of the correction of the bomb- ^{14}C
15 or the Suess effect. Surface water sinking into the interior of the ocean in high latitudes, however, are known to have an initial ^{14}C -age up to 900 yr older than tropical and subtropical surface waters (Bard, 1988). Hence ^{14}C -ages in the interior ocean are not real, are not reflecting the passage time in the interior of the ocean, but are apparent ages only (e.g. Broecker, 1979).

In the context of ocean biogeochemistry the time elapsed since the last contact of a water parcel with the atmosphere, i.e. water of age zero, is of particular interest. For example, the estimation of rates of ocean respiration or CaCO_3 -dissolution from cumulative tracer changes requires corrected reliable age determinations (Jenkins, 1982; Sarmiento et al., 1990; Feely et al., 2002). ^{14}C -ages of several hundred years for waters actually in contact with the atmosphere can thus pose a severe problem. Inferring true ages from ^{14}C -ages in the interior of the ocean obviously requires a correction for the “initial-age” effect before they can be used to derive the time component of circulation (Broecker, 1979; Bard, 1988; Campin et al., 1999). The term “bulk ^{14}C -age” is used here to denote those ages computed from the distribution of natural ^{14}C -DIC not
25

GMDD

7, 7033–7074, 2014

^{14}C -age tracers in global ocean circulation models

W. Koeve et al.

Title Page

Abstract

Introduction

Conclusions

References

Tables

Figures



Back

Close

Full Screen / Esc

Printer-friendly Version

Interactive Discussion



**¹⁴C-age tracers in
global ocean
circulation models**

W. Koeve et al.

Title Page

Abstract

Introduction

Conclusions

References

Tables

Figures



Back

Close

Full Screen / Esc

Printer-friendly Version

Interactive Discussion



primitive-equation model (Marshall et al., 1997). The coarse resolution matrix (hereafter MIT2.8) was derived from a $2.8^\circ \times 2.8^\circ$ global configuration of this model with 15 vertical layers, forced with monthly mean climatological fluxes of momentum, heat, and freshwater, and subject to a weak restoring of surface temperature and salinity to observations. The higher resolution matrix (hereafter ECCO) is based on the data-assimilation model of the ECCO-consortium (Estimating the Circulation and Climate of the Ocean; Stammer et al., 2004) and has a horizontal resolution of $1^\circ \times 1^\circ$ and 23 vertical layers. For details see Khatiwala (2007) and Kriest et al. (2010, 2012). Wind-speed dependence of gas exchange applies winds from Trenberth et al. (1989) with a monthly resolution regridded to the respective model grid. Sea-ice fields applied are the OCMIP-2 ice mask (Orr et al., 1999) for MIT2.8 and NASA ISLSCP climatology (http://iridl.ldeo.columbia.edu/SOURCES/.NASA/.ISLSCP/.GDSLAM/.Snow-Ice-Oceans/.sea/.sea_ice/) for ECCO (S. Dutkiewics, MIT, personal communication, 2011). OCMIP is the Ocean Carbon cycle Model Intercomparison Project (<http://ocmip5.ipsl.jussieu.fr/OCMIP/>).

The third model used is the University of Victoria Earth System Climate Model (UVIC; Weaver et al., 2001), version 2.8 in the configuration used at GEOMAR (Oschlies et al., 2008). The ocean component of this model is a coarse-resolution ($1.8^\circ \times 3.6^\circ$, 19 vertical layers) 3-D-ocean general-circulation model (MOM2). Wind velocities are prescribed from the NCAR/NCEP monthly climatology. Sea-ice coverage is computed from a dynamic/thermodynamic sea-ice model (Bitz et al., 2001). The biogeochemical ocean model of the UVIC is described in detail by Schmittner et al. (2008).

For the ¹⁴C-simulations with the TMM models we largely follow the OCMIP-2 protocol (Orr et al., 1999) and study the natural ¹⁴C-distribution in an abiotic setting and against an atmosphere of $\Delta^{14}\text{C} = 0$ and a constant $p\text{CO}_2^{\text{atm}} = 280 \mu\text{atm}$. DIC and ¹⁴C-DIC are prognostic model tracers of total dissolved CO_2 and ¹⁴ CO_2 respectively. Alkalinity is prescribed from the model's salinity field assuming a fixed alkalinity / salinity ratio. Like in other ¹⁴C modelling studies, biotic fluxes are ignored following Fiadeiro (1982). All model runs were integrated for several thousand years and can be considered

equilibrium runs. For UVIC the ^{14}C -simulations are made alongside a normal, biotic model run.

Air-sea exchange of CO_2 and $^{14}\text{CO}_2$ in all three models is treated according to Eqs. (1) and (2).

$$5 \quad \text{CO}_2(\text{ex}) = (1 - \text{ice}) \cdot k_w \cdot (\text{CO}_{2(\text{water})}^* - \text{CO}_{2(\text{air})}^*) \quad (1a)$$

$$^{14}\text{CO}_2(\text{ex}) = (1 - \text{ice}) \cdot k_w \cdot (\text{CO}_{2(\text{water})}^* \cdot R_{(\text{water})} - \text{CO}_{2(\text{air})}^* \cdot R_{(\text{atm})}) \quad (1b)$$

$$k_w = a \cdot U^n \cdot (\text{Sc}/660)^{-\eta} \quad (2)$$

$$10 \quad \text{with } \text{CO}_{2(\text{air})}^* = \text{CO}_{2(\text{sol})} \cdot p\text{CO}_{2(\text{atm})} \cdot P_{(\text{atm})}.$$

k_w is the gas transfer velocity, U is wind speed, $n = 2$, Sc is the Schmidt number, and $\eta = 0.5$. $\text{CO}_{2(\text{water})}^*$ is the sum of CO_2 dissolved in seawater and H_2CO_3 in surface water computed in carbon-cycle models from the DIC concentration and an estimate of pH (e.g. Follows et al., 2006). $\text{CO}_{2(\text{air})}^*$ is the equilibrium CO_2 concentration given atmospheric $p\text{CO}_2$, CO_2 solubility, and the local atmospheric pressure; $\text{CO}_{2(\text{sol})}$ is the solubility of CO_2 , $p\text{CO}_{2(\text{atm})}$ is CO_2 partial pressure in the atmosphere, $P_{(\text{atm})}$ is the local atmospheric pressure, $R_{(\text{atm})}$ is the $^{14}\text{C}/\text{C}$ ratio of the atmosphere and $R_{(\text{water})}$ is the $^{14}\text{C}/\text{C}$ ratio of the surface water. In the standard configuration the gas transfer velocity k_w is computed using a value of $a = 0.337$, following the OCMIP-2 protocol. The term “ice” represents the fraction of water area covered by sea ice.

In the ocean the bulk ^{14}C -age (in units of years) can be computed (Stuiver and Polach, 1977) according to Eq. (3):

$$^{14}\text{C}\text{-age} = -8033 \log_e(\Delta^{14}\text{C}/1000 + 1) \quad (3)$$

2.2 Model tracers

25 In order to study the distribution of preformed ^{14}C in the interior of the ocean, we design a suite of additional model tracers.

Title Page

Abstract

Introduction

Conclusions

References

Tables

Figures



Back

Close

Full Screen / Esc

Printer-friendly Version

Interactive Discussion



¹⁴C-age tracers in global ocean circulation models

W. Koeve et al.

Title Page

Abstract

Introduction

Conclusions

References

Tables

Figures



Back

Close

Full Screen / Esc

Printer-friendly Version

Interactive Discussion



1. $^{14}\text{C-DIC}^{\text{bulk}}$: this is the tracer of natural $^{14}\text{C-DIC}$ implemented following the OCMIP2 protocol. The age computed from this tracer via Eq. (3) has also been called “conventional $^{14}\text{C-age}$ ” (Khatiwala et al., 2012) but is usually referred to as $^{14}\text{C-age}$ or radiocarbon age. We will use the term $^{14}\text{C-age}^{\text{bulk}}$ or bulk $^{14}\text{C-age}$ in order to highlight the fact that it consists of several components (see below).
2. $\text{age}^{\text{ideal}}$: a tracer of the time elapsed since the last contact with atmosphere. The “ideal age” model tracer (Thiele and Sarmiento, 1990; England, 1995; England and Maier-Reimer, 2001) works like a clock counting time after being restored to zero, which happens every time the water resides at the surface. Everywhere else it ages with a rate of 1 day day^{-1} and is subject to mixing and advection in the interior of the ocean. Synonyms of the age measured by this tracer used in the scientific literature include: “circulation age” (Matsumoto, 2007; Khatiwala et al., 2012), “ventilation age” (Adkins and Boyle, 1997; Campin et al., 1999), and “ideal age” (Thiele and Sarmiento, 1990).
3. $^{14}\text{C-DIC}^{\text{pre}}$: a preformed $^{14}\text{C-DIC}$ tracer is restored to the model’s actual $^{14}\text{C-DIC}$ at the surface while in the interior of the ocean it is only mixed and advected but is not subject to radioactive decay. The respective preformed ^{14}C age (yr) is computed from $^{14}\text{C-age}^{\text{pre}} = -8033 \cdot \log_e(^{14}\text{C-DIC}^{\text{pre}} / \text{DIC}^{\text{pre}})$, where DIC^{pre} is preformed total CO_2 . Note that in an abiotic run DIC^{pre} is always equal to DIC .
4. $^{14}\text{C-DIC}^{\text{decay}}$: a $^{14}\text{C-DIC-decay}$ tracer is set to zero in surface waters and adds up any $^{14}\text{C-decay}$ of the $^{14}\text{C-DIC}$ tracer in the interior of the ocean. It is also advected and mixed in the interior of the ocean. The $^{14}\text{C-decay}$ age (yr) is computed from $^{14}\text{C-age}^{\text{decay}} = -8033 \cdot \log_e[(\text{DIC} + ^{14}\text{C-DIC}^{\text{decay}}) / \text{DIC}]$.
5. age^{pre} : in order to simplify the comparison between the ideal-age tracer and the age computed from the $^{14}\text{C-DIC}$ tracer, we design another tracer of preformed $^{14}\text{C-age}$. This tracer (age^{pre}) has units of time. At the surface it is assigned the bulk $^{14}\text{C-age}$, which is computed at any time step during model runtime from $^{14}\text{C}/\text{C}$

ratios. In the interior of the ocean this tracer is advected and mixed like all other tracers, but it does not age. While tracer $^{14}\text{C-DIC}^{\text{pre}}$ (3) is one of concentration, age^{pre} is one of time.

6. age^{bulk} : finally, we design an explicit tracer which combines the behaviour of the age^{pre} tracer at the surface and the ideal age tracer ($\text{age}^{\text{ideal}}$) in the interior of the ocean. At the surface age^{bulk} is assigned the bulk ^{14}C -age, which is computed at any time step during model runtime from $^{14}\text{C}/\text{C}$ ratios. In the ocean interior it ages with a rate of 1 day day^{-1} and is subject to mixing and advection.

This provides us with a duplicate set of tracers (Table 1) describing the preformed component, the circulation component and bulk age, with one set of the tracers based on ^{14}C , the other not. Where the complete set of tracers is involved we present and discuss results from the ECCO model. The tracers $^{14}\text{C-DIC}^{\text{bulk}}$ and $\text{age}^{\text{ideal}}$ are implemented in all three models.

2.3 Model experiments

Reference model runs are carried out with all three models. We apply a gas transfer constant of $a = 0.337$, wind fields and ice cover as given in Sect. 2.1 for these runs. Implemented tracers are DIC, $^{14}\text{C-DIC}^{\text{bulk}}$ and $\text{age}^{\text{ideal}}$. We use these tracers to approximate the preformed component of bulk ^{14}C -age in the different models by diagnosing it during post processing from the difference of ^{14}C -age^{bulk} and $\text{age}^{\text{ideal}}$ (see Sect. 3.1 for the results). Reference runs also serve as spin-up runs from which other model experiments are initialised.

In a second set of experiments we implement DIC and all six tracers described in Sect. 2.2. We will use this combination of tracers to fully quantify the non-linearity arising from mixing of $^{14}\text{C-DIC}$ and DIC tracers, respectively, on computed ^{14}C -age components. We present and discuss results from the ECCO model in Sect. 3.2.

We perform several sensitivity experiments (Results see Sect. 3.3) with the objective to study the sensitivity of the preformed ^{14}C -age distribution to relevant model

^{14}C -age tracers in global ocean circulation models

W. Koeve et al.

Title Page

Abstract

Introduction

Conclusions

References

Tables

Figures



Back

Close

Full Screen / Esc

Printer-friendly Version

Interactive Discussion



**¹⁴C-age tracers in
global ocean
circulation models**

W. Koeve et al.

Title Page

Abstract

Introduction

Conclusions

References

Tables

Figures



Back

Close

Full Screen / Esc

Printer-friendly Version

Interactive Discussion



parameters. All sensitivity experiments are carried out with the reduced set of model tracers (i.e. $^{14}\text{C-DIC}^{\text{bulk}}$ and ideal age tracer, Table 1) and we diagnose the preformed ^{14}C -age offline during post-processing of model output. This procedure is justified by results presented in Sect. 3.2. Using all models, we repeat the standard experiment with a reduced gas exchange rate. For this purpose we reduce the standard value of the gas transfer constant from $a = 0.337$ to a value of $a = 0.24$ (see Eq. 2). These experiments are motivated by uncertainties of this constant (Sweeney et al., 2007). In order to study the impact of ice cover on preformed ^{14}C -age, we perform one model run with the ECCO-model, prescribing the value of “ice” in Eq. (1) to zero.

Further, we estimate the residence time of the surface layer in two model runs (ECCO, MIT2.8). For this purpose we modify the definition of our ideal age tracer such that it is set to zero everywhere below a model specific reference depth and allowed to age in layers higher up. The reference depths are 135 m in ECCO and 120 m in MIT2.8. The idea here is to have a reference depth larger than 100 m, a depth often used pragmatically to define the productive surface layer. Differences between the reference depths are due to the different vertical resolutions of the models.

Finally, we perform a series of case studies to study the sensitivity of ^{14}C -age^{bulk}, age^{ideal} and the diagnosed preformed ^{14}C -age to the choice of vertical diffusivity in a model (see Sect. 4 for the results). The intensity of diapycnal mixing in the ocean is one of the key controls of ocean circulation and biogeochemical cycles (Bryan, 1987). For the experimental design we follow Duteil and Oschlies (2011), who used UVIC 2.8. Here, we apply the Kiel-Version of UVIC 2.9 (Keller et al., 2012) to which we added an ideal age tracer. We perform eight sensitivity runs assuming background mixing coefficients of $K_v = 0.01, 0.05, 0.1, 0.15, 0.2, 0.3, 0.4, 0.5 \text{ cm}^2 \text{ s}^{-1}$. Following Duteil and Oschlies (2011) a value of $1 \text{ cm}^2 \text{ s}^{-1}$ is added to the background diffusivity south of 40° S to account for observed vigorous mixing in the Southern Ocean. Each of the model experiments has been integrated for 10 000 yr under preindustrial atmospheric and astronomical boundary conditions, i.e. all model runs assume constant atmospheric $\Delta^{14}\text{C} = 0$ and $p\text{CO}_2$ of 280 μatm .

3 Principal components of bulk ^{14}C age

3.1 Ideal age and bulk ^{14}C -age distribution in three ocean models and the concept of preformed ^{14}C -age

We first compare global mean profiles of bulk ^{14}C -ages and ideal ages (Fig. 2a). A number of features is evident. First, bulk ^{14}C -ages are much larger than the ideal ages in any model. The global mean offset between the two age measures varies by up to a factor of two between models (Fig. 2b). In the deep ocean the offset is about 400 yr in MIT2.8 and 680 yr (800 yr) in ECCO (UVIC), respectively. The age offset may be either rather homogeneous vertically (MIT2.8) or have a marked vertical gradient of up to 400 yr difference between surface and deep water (ECCO and UVIC). Secondly, global mean surface bulk ^{14}C -ages are smaller than the data-based estimate from GLODAP in all three models (Fig. 2a). Thirdly, a model judgement based just on global mean profiles of bulk ^{14}C -ages would indicate that over most of the ocean the UVIC model is the one in best agreement with observations. Furthermore, one might conclude that the MIT2.8 model appears to have too young waters, and presumably too vigorous a circulation, almost everywhere.

Interestingly, the ideal age tracer indicates just the opposite. Deep-ocean MIT2.8 waters have highest ages pointing to a more sluggish circulation while in UVIC (and ECCO) deep-ocean waters are in fact younger, indicating a more vigorous circulation compared to the MIT2.8 model. Finally, in the upper 2000 m, the global mean profiles of the ideal age tracer suggest the circulations to be similar in all three models, at least much more similar than the bulk ^{14}C -ages indicate.

In conjunction with the observation that ocean/atmosphere ^{14}C -equilibration is slow (Broecker and Peng, 1974) and surface-ocean bulk ^{14}C -ages are well above zero (see Fig. 1b), we suspect that (most of) the difference between bulk ^{14}C -ages and ideal ages in the interior of the ocean is due to the bulk ^{14}C -age which a water mass had at the time entering into the ocean's interior, i.e. its preformed ^{14}C -age.

GMDD

7, 7033–7074, 2014

**^{14}C -age tracers in
global ocean
circulation models**

W. Koeve et al.

Title Page

Abstract

Introduction

Conclusions

References

Tables

Figures



Back

Close

Full Screen / Esc

Printer-friendly Version

Interactive Discussion



3.2 Effects of tracer mixing on age estimates

In the following we will use dedicated model experiments carried out with only the ECCO model, in order to quantify the relative importance of the three terms on the right-hand side of Eq. (4). To explore the mixing term in more detail, we first apply the additional tracers $^{14}\text{C-DIC}^{\text{pre}}$ and $^{14}\text{C-DIC}^{\text{decay}}$ (Table 1). In addition to the DIC, $^{14}\text{C-DIC}$, and ideal age tracers we add an explicit preformed $^{14}\text{C-DIC}$ tracer ($^{14}\text{C-DIC}^{\text{pre}}$) and an explicit $^{14}\text{C-DIC}$ -decay tracer ($^{14}\text{C-DIC}^{\text{decay}}$). We initialize these tracers from model output of the spin-up run with the DIC, $^{14}\text{C-DIC}$ and ideal-age tracers pretending the “mixing residual” term of Eq. (4) to be zero everywhere. Running the model for another 2500 yr, we find the sum of the preformed and the decay tracers to match the $^{14}\text{C-DIC}$ tracer perfectly (Fig. 4a). The sum of ages ($^{14}\text{C-age}^{\text{pre}} + ^{14}\text{C-age}^{\text{decay}}$), however, is on average 6 % smaller than the age computed from the $^{14}\text{C-DIC}^{\text{bulk}}$ tracer (Fig. 4b).

The difference between Fig. 4a and b, i.e. the low bias in ages computed from ^{14}C -tracers relative to the tracer itself, is explained by the combination of the logarithmic transformation in the age computation (Eq. 3) and the effect of mixing of waters with different $^{14}\text{C}/\text{C}$ tracer ratios (Khaliwala et al., 2001, 2012). To exemplify the principal process at work consider a system of two water masses of different age, which are mixed instantaneously along a linear mixing line. The relationship of $^{14}\text{C-DIC}$ tracer vs. ideal age is linear while the relationship of bulk $^{14}\text{C-age}$ vs. ideal age is not (Fig. 5) due to the logarithmic decay of ^{14}C . Computed ^{14}C -ages are always smaller than the correct age of the mixture. The magnitude of this mixing effect depends on the age difference of the water masses involved. In the three-dimensional situation of the ocean, mixing is much more complex than in this simple example; usually more than two water masses are involved, mixing is not instantaneous, and isopycnal and diapycnal mixing are superimposed. To make this effect visible and quantifiable in our model, we compare age estimates from two sets of tracers (Table 1) tracking (a) the circulation component of age, (b) preformed age, and (c) bulk age. One set of these tracers

Title Page

Abstract

Introduction

Conclusions

References

Tables

Figures



Back

Close

Full Screen / Esc

Printer-friendly Version

Interactive Discussion



**¹⁴C-age tracers in
global ocean
circulation models**

W. Koeve et al.

Title Page

Abstract

Introduction

Conclusions

References

Tables

Figures



Back

Close

Full Screen / Esc

Printer-friendly Version

Interactive Discussion



behaves ideally in the interior of the ocean, in the sense that where they are affected by mixing, the mixing products can be described by mixing along a linear mixing line. These tracers are the age^{ideal}, age^{pre}, and age^{bulk} tracers (Table 1). The latter two tracers inherit the age of ¹⁴C-age^{bulk} at the surface, while in the interior of the ocean they behave like ideal tracers, being either only transported (age^{pre} tracer) or being both transported and aging with a rate of 1 day day⁻¹ (age^{bulk} tracer). We compare ages derived from these ideally-behaving tracers and the respective ages from the ¹⁴C-based tracers, ¹⁴C-age^{decay}, ¹⁴C-age^{pre}, and ¹⁴C-age^{bulk}. In all three cases (circulation component of age, preformed component of age and bulk age) we see that ¹⁴C-based ages underestimate their ideally-behaving tracer counterparts. We present the results as anomalies (ideally behaving – ¹⁴C-based) of ages along the combined section through the Atlantic (30° W), Southern (60° S) and Pacific (140° W) Oceans (Fig. 6). The age anomaly age^{bulk} – ¹⁴C-age^{bulk} (Fig. 6a) is close to zero in the surface ocean, in the northern North Atlantic, and in the Atlantic sector of the Southern Ocean. Away from these outcrop regions and largely following increasing ideal age (age^{ideal}) the anomaly increases to maximum values of about 50 yr in the (South) Atlantic Ocean and about 80 yr in the (North) Pacific Ocean. This difference is moderate and equivalent to a few percent of the bulk ¹⁴C-age. Preformed ages (Fig. 6b) show very small anomalies (age^{pre} – ¹⁴C-age^{pre}) of only a few years (and usually less than 1 % of age^{pre}), again with maxima in the South Atlantic Ocean and the North Pacific Ocean. The largest difference is found between age^{ideal} and ¹⁴C-age^{decay}. In the deep northern North Pacific this difference is almost 200 yr (Fig. 6c). Over much of the Pacific Ocean it is equivalent to about 15 % of ideal age.

The small difference age^{bulk} – ¹⁴C-age^{bulk} (Fig. 6a) in combination with an almost perfect behaviour of the preformed age tracers (Fig. 6b) suggests that our initial assumption (Sect. 3.1, Fig. 2) that the preformed age can be well approximated by (Eq. 5) the difference between the bulk ¹⁴C-age and the ideal age of a model is justified.

$$\text{preformed } ^{14}\text{C-age} \approx \text{bulk } ^{14}\text{C-age} - \text{ideal age} \quad (5)$$

In any case, preformed ^{14}C -ages estimated from this difference provide a conservative, lower-limit estimate of preformed age. In the ECCO model, this underestimate may be as large as 20 % in individual grid boxes (Fig. 4c). On average, however, it is about 7 % with higher values observed towards the North Pacific Ocean. This uncertainty is small given the order of 50 % contribution of the preformed age to bulk ^{14}C -ages presented in Sect. 3.1. For the sake of saving computational time by having a reduced number of tracers, we hence ignore the “mixing effect” in the following section where we discuss a series of sensitivity runs.

3.3 Mechanisms controlling preformed ^{14}C -age

In this section we treat the major processes, which determine the magnitude of preformed ^{14}C -age and how they influence model assessment if based on bulk ^{14}C -ages. In this section preformed ^{14}C -age is diagnosed offline during post processing from model output using Eq. (5). Bulk ^{14}C -ages of several hundred years in the surface ocean (Fig. 1b) have been attributed to the long equilibration times of carbon isotopes (Broecker and Peng, 1974). While for CO_2 the equilibration time is governed by the product of the time scale of gas exchange (order of one month) and the ratio $\text{CO}_3^{2-}/\text{CO}_2^{\text{aq}}$ (10–15 in the surface ocean), the equilibration time of carbon isotopes scales with the ratio $\text{TCO}_2/\text{CO}_2^{\text{aq}}$. Since there is about ten times more total CO_2 than carbonate ions in seawater, the equilibration time of carbon isotopes is larger by about a factor of ten, i.e. of the order of a decade (Broecker and Peng, 1974). The residence time of waters at the ocean surface is usually much shorter, and equilibrium with atmospheric ^{14}C is therefore not attained. In our MIT2.8 model, for example, surface water residence times with respect to a global source depth domain below 120 m water depth range up to two years in subpolar and most northern-hemisphere polar waters, up to five years in Southern Ocean polar waters and equatorial upwelling regions, and up to 7 years in the subtropical gyres (Fig. 7). In the ECCO model residence times in the Southern Ocean are even shorter. In general, in areas of deep convection or

Title Page

Abstract

Introduction

Conclusions

References

Tables

Figures



Back

Close

Full Screen / Esc

Printer-friendly Version

Interactive Discussion



coverage, (d) water residence time in the surface of the region of water mass formation, and (e) the relative contribution of different source water regions (e.g. NADW and AABW) to the total deep water formation rate.

The gas-exchange formulation (Eqs. 1–3) is essentially identical in all three tested models. In particular all models apply wind speed squared and the OCMIP2 gas transfer constant of 0.337. This value is based on tuning one model of the OCMIP2 family against the bomb ^{14}C ocean inventory estimated from observations (Broecker et al., 1985) and considered correct at the time of the OCMIP2 experiment. Evidence has since accumulated suggesting that the bomb ^{14}C ocean inventory is in fact smaller by about 25 % (Sweeney et al., 2007). As a consequence, the gas transfer constant must be reduced by the same fraction. Such a change in the gas transfer constant has little effect on net oxygen or total- CO_2 fluxes between ocean and atmosphere. It has, however, a considerable effect on preformed ^{14}C -age and hence also the bulk ^{14}C -age distribution in the ocean. Assuming a value of 0.24 instead of 0.337, the global mean profiles of preformed ^{14}C -ages (Fig. 8a) increase by about 150 (ECCO, UVIC) to 200 (MIT2.8) yr. In the global mean profile this shift is almost constant with depth. Concerning the global mean profiles of bulk ^{14}C -ages, two features are evident (Fig. 8b). First, model surface values are now ($a = 0.24$) much closer to bulk ages derived from the “observed” natural ^{14}C as compared to our reference runs ($a = 0.337$; Fig. 2a). Reducing the gas transfer constant hence solves one of the model-data comparison issues discussed in Sect. 3.1 (Fig. 2a). At depth (ignoring the deepest layers below 4000 m) this increase shifts the global mean profile of the MIT2.8 much closer to observations. With the reduced gas exchange constant the bulk ^{14}C -ages of the UVIC model appear to be too large compared to observations and the ECCO model appears to be the best performing model in our model intercomparison exercise. ^{14}C -based judgement of model circulation obviously is very sensitive to the air–sea exchange formulation, which, however, only affect preformed age, not ideal age. Using an improper gas exchange formulation may hence adversely affect the interpretation of ^{14}C -model experiments concerning a model’s circulation dynamics. In fact, this is occasionally

^{14}C -age tracers in global ocean circulation models

W. Koeve et al.

Title Page

Abstract

Introduction

Conclusions

References

Tables

Figures



Back

Close

Full Screen / Esc

Printer-friendly Version

Interactive Discussion



seen in the literature (e.g. Cao and Jain, 2005; their Fig. 8d). One potential solution to this problem is to select the most suitable gas exchange constant for a given model and wind field by performing a bomb- ^{14}C calibration experiment (Sweeney et al., 2007).

Ice coverage is another factor potentially influencing gas equilibration at deep-water formation sites (Ito et al., 2004; Duteil et al., 2013). Ito et al. (2004) reported ice cover to be responsible for about a third of the oxygen disequilibrium observed in their model. In order to test the effect of ice cover on ^{14}C gas exchange and on the magnitude of preformed ^{14}C -age, ice cover was switched off for 6000 yr (Fig. 9). This reduced preformed ^{14}C -age by up to 70 yr, or less than 10% of its normal value. Ice cover hence appears not to be of major importance in controlling preformed ^{14}C -ages.

4 Case studies

The overall importance, but also the inter-model variability, of the preformed ^{14}C -age is evident from Fig. 10. The preformed ^{14}C -age over much of the ocean contributes to bulk ^{14}C -age by about 50% in UVIC and ECCO, with higher shares in young water in the upper ocean in all models. In MIT2.8 this fraction is smaller in the deep ocean (about 30%) (Fig. 10a). In all models, the relative importance of the preformed age component decreases with distance from the deep-water formation regions (Fig. 10b).

In order to demonstrate the adverse effects of neglecting the preformed component of ^{14}C -age we give two examples in the following. In the first example we consider the age of waters in the oxygen minimum zone of the Pacific Ocean. Duteil and Oschlies (2011) recently studied the sensitivity of the volume and age of suboxic waters to the choice of the vertical diffusivity constant (K_v) in a model (UVIC). Using UVIC 2.8, they found dome-shaped distributions for both volume and age. Maximum suboxic volume and ^{14}C -age^{bulk} were found at an intermediate K_v of $0.2 \text{ cm}^2 \text{ s}^{-1}$ (Duteil and Oschlies, 2011, their Fig. 1b). Repeating these experiments with the Kiel-Version of UVIC 2.9 (Keller et al., 2012) to which we added an ideal age tracer, we find a very similar distribution with the ^{14}C -age^{bulk} maximum also at $K_v = 0.2 \text{ cm}^2 \text{ s}^{-1}$ (Fig. 11a). At the highest

Title Page

Abstract

Introduction

Conclusions

References

Tables

Figures



Back

Close

Full Screen / Esc

Printer-friendly Version

Interactive Discussion



**¹⁴C-age tracers in
global ocean
circulation models**

W. Koeve et al.

Title Page

Abstract

Introduction

Conclusions

References

Tables

Figures



Back

Close

Full Screen / Esc

Printer-friendly Version

Interactive Discussion



(lowest) tested K_V values of 0.5 (0.01) $\text{cm}^2 \text{s}^{-1}$ the mean bulk ^{14}C -age is lower by 90 (70) yr. Separating bulk age into its circulation component (ideal age tracer) and its preformed component (^{14}C -age^{bulk} – age^{ideal}) we find, however, very little sensitivity of age^{ideal} to K_V between 0.01 and 0.3. Only for high K_V (0.3 to $0.5 \text{ cm}^2 \text{ s}^{-1}$) we find that the sensitivity of ^{14}C -age^{bulk} is to a large extent due to changes in the circulation component of the age (Fig. 11b). For K_V values below $0.2 \text{ cm}^2 \text{ s}^{-1}$ more than 60 % of the gradient of ^{14}C -age^{bulk} (over K_V) is from the preformed component (Fig. 11c). The similarity of patterns of suboxic volume and ^{14}C -age^{bulk} led Duteil and Oschlies (2011) to conclude that their model results confirm the notion of a predominant control of suboxic water volume by ocean dynamics rather than by local export production and remineralisation. In quantitative terms, and for our model experiments, the suboxic volume appears to be linearly correlated with ^{14}C -age^{bulk} (Fig. 11d). Variations of ^{14}C -age^{bulk} explain 65 % (93 %) of the variation of suboxic volume in the Eastern Tropical Pacific above 1000 m with $n = 8$ ($n = 7$, excluding the lowest value $K_V = 0.01$), respectively. In fact the relationship of suboxic volume and age^{ideal} is not tight and does not confirm the simple physical control of suboxic volume (Fig. 11e). A linear correlation explains only about 18 % of suboxic volume variations by the model's ideal age, i.e. the circulation component of ^{14}C -age.

In the second example we explore N–S age gradients in the deep Atlantic Ocean. The mean ^{14}C -age^{bulk} of waters below 1500 m in the Atlantic Ocean shows a marked N–S gradient, with higher values in the Southern Ocean. The slope of this gradient is highly sensitive to the choice of K_V in the model (Fig. 12a; see also Fig. 3). Ideal age also shows a sensitivity to K_V , but the patterns are very different with highest sensitivity in the tropics and lowest sensitivity in the northern North Atlantic (Fig. 12b). In fact, the patterns observed in ^{14}C -age^{bulk} are largely due to the sensitivity of the preformed component (Fig. 12c) to K_V . Compared with the run with the highest K_V , the southern end member of preformed ^{14}C -age of the lowest K_V run is almost twice as high (Fig. 13a–c). These differences appear to be largely due to strong differences in the

maximum bulk age observed in the different model runs in the North Pacific (Fig. 14). With low K_v , the deep North Pacific shows a ^{14}C -age^{bulk} of up to 3000 years while with high K_v , this age is about 1500 yr only. It is the upwelling of these ^{14}C -depleted waters in the Southern Ocean, which strongly impacts the southern end member of waters ventilating the South Atlantic. The northern end member contributes much less to the K_v sensitivity of age gradients in the deep Atlantic (Fig. 12).

5 Conclusion

Globally, bulk ^{14}C -age is dominated by two equally important components, one associated with the time elapsed since last contact with the atmosphere and one associated with a preformed age related to the slow and incomplete atmospheric equilibration of ^{14}C in the surface ocean. While on average the preformed component accounts for about 50 % of the bulk ^{14}C -age, there is large variability. Regionally and within a given model the relative contribution is up to 100 % near the ocean's surface, but is well below 50 % in the oldest, deep waters, typically observed in the deep North Pacific Ocean. Regional variability, e.g. in the deep Atlantic Ocean, where it is associated with mixing of end members with very different preformed ^{14}C -age, can well mask the circulation component such that it is not visible from the distribution of bulk ^{14}C -age, alone. Between models, the variability can also be considerable, likely due to an interplay of physical model parameters (e.g. diapycnal diffusivity, K_v) influencing the circulation dynamics within the ocean, and those that control gas exchange of ^{14}C with the atmosphere, like the gas exchange constant, ice coverage, or the wind fields used. In our comparison of three different models the choice of the gas exchange constant (parameter a in Eq. 2) from a parameter range within current uncertainty may either yield the UVIC model (Fig. 2a) or the ECCO model (Fig. 8b) to best compare with observed bulk ^{14}C -age. This is solely due to its impact on the preformed ^{14}C -age component and not related to the models circulation. A data-based evaluation and tuning of a model's

Title Page

Abstract

Introduction

Conclusions

References

Tables

Figures



Back

Close

Full Screen / Esc

Printer-friendly Version

Interactive Discussion



circulation which uses ^{14}C -age^{bulk} without considering the variability of preformed ^{14}C -age is hence at risk to select for the wrong circulation.

In the similar way, temporal changes (e.g. over glacial–interglacial cycles) of the deep ocean ^{14}C -age distributions may be misunderstood if the bulk ^{14}C -age is not corrected properly for the preformed component. For paleo-reconstructions the bulk ^{14}C -age of the deep ocean is preserved in the shells of benthic foraminifera and the surface ocean ^{14}C -distribution (i.e. the surface distribution of preformed ^{14}C -age) in their pelagic counterparts (Bard, 1988). However, the deep ocean distribution of preformed ^{14}C -age is very difficult to quantify since the actual mixing ratios of end members with different preformed ^{14}C -ages will change along with a changing circulation (Campin et al., 1999) and is not known for time periods other than the present. For the glacial period, for example, waters in the deep South Atlantic Ocean appeared older (older ^{14}C -age^{bulk}) compared with late Holocene experiments in a model study. The ideal deal age however was younger. The bias towards old ^{14}C -age^{bulk} was from the increased invasion of Antarctic bottom water with a large preformed ^{14}C -age (Campin et al., 1999).

The third component of bulk ^{14}C -age, which is associated with the logarithmic decay of ^{14}C , has been quantified in detail in this study. It was found to be generally relatively small, in particular compared to the other two. We propose that in models the preformed component can be estimated from the difference of bulk ^{14}C -age and the model's ideal age (see Eq. 5). There is no straightforward ideal age tracer in the real ocean though. Recent studies, however, have tried to construct an equivalent from a multi tracer analysis (e.g. Khatiwala et al., 2012). These data products will be very helpful together with the distribution of natural ^{14}C (GLODAP and GLODAP-2) to support data-based model evaluation. Model studies of ocean circulation and biogeochemical processes will benefit from this.

The general form of Eq. (5) is similar to equations describing the principal components of e.g. phosphate and oxygen in the ocean. The observed phosphate concentration at any point in the ocean can be described as the sum of preformed phosphate and phosphate remineralised from decaying organic matter. Similarly, the observed

^{14}C -age tracers in global ocean circulation models

W. Koeve et al.

Title Page

Abstract

Introduction

Conclusions

References

Tables

Figures



Back

Close

Full Screen / Esc

Printer-friendly Version

Interactive Discussion



**¹⁴C-age tracers in
global ocean
circulation models**

W. Koeve et al.

Title Page

Abstract

Introduction

Conclusions

References

Tables

Figures



Back

Close

Full Screen / Esc

Printer-friendly Version

Interactive Discussion



- Broecker, W. S., Peng., T.-H., Ostlund, H. G., and Stuiver, M.: The distribution of bomb radiocarbon in the ocean, *J. Geophys. Res.*, 90, 6953–6970, 1985.
- Bryan, F.: Parameter sensitivity of primitive equation ocean general circulation models, *J. Phys. Oceanogr.*, 17, 970–985, 1987.
- 5 Caldeira, K., Wickett, M. E., and Duffy, P. B.: Depth, radiocarbon, and the effectiveness of direct CO₂ injections as an ocean carbon sequestration strategy, *Geophys. Res. Lett.*, 29, 1766, doi:10.1029/2001GL014234, 2002.
- Campin, J.-M., Fichet, T., and Duplessy, J.-C.: Problems with using radiocarbon to infer ocean ventilation rates for past and present climates, *Earth Planet. Sc. Lett.*, 165, 17–24, 1999.
- 10 Cao, L. and Jain, A.: An Earth system model of intermediate complexity: simulations of the role of ocean mixing parameterizations and climate change in estimated uptake for natural and bomb radiocarbon and anthropogenic CO₂, *J. Geophys. Res.*, 110, C09002, doi:10.1029/2005JC002919, 2005.
- DeVries, T. and Primeau, F.: Dynamically and observationally constrained estimates of water-mass distributions and ages in the global ocean, *J. Phys. Oceanogr.*, 41, 2381–2401, doi:10.1175/JPO-D-10-05011.1, 2011.
- Druffel, E. M.: Radiocarbon in annual coral rings from the eastern tropical pacific ocean, *Geophys. Res. Lett.*, 8, 59–62, 1981.
- Duteil, O. and Oschlies, A.: Sensitivity of simulated extent and future evolution of marine suboxia to mixing intensity, *Geophys. Res. Lett.*, 38, L06607, doi:10.1029/2011GL046877, 2011.
- 20 Duteil, O., Koeve, W., Oschlies, A., Aumont, O., Bianchi, D., Bopp, L., Galbraith, E., Matear, R., Moore, J. K., Sarmiento, J. L., and Segsneider, J.: Preformed and regenerated phosphate in ocean general circulation models: can right total concentrations be wrong?, *Biogeosciences*, 9, 1797–1807, doi:10.5194/bg-9-1797-2012, 2012.
- 25 Duteil, O., Koeve, W., Oschlies, A., Bianchi, D., Galbraith, E., Krist, I., and Matear, R.: A novel estimate of ocean oxygen utilisation points to a reduced rate of respiration in the ocean interior, *Biogeosciences*, 10, 7723–7738, doi:10.5194/bg-10-7723-2013, 2013.
- Emerson, S. R. and Hedges, J. I.: *Chemical Oceanography and the Marine Carbon Cycle*, Cambridge University Press, Cambridge, 453 pp., 2008.
- 30 England, M. H.: The age of water and ventilation timescales in a global ocean model, *J. Phys. Oceanogr.*, 25, 2756–2777, 1995.
- England, M. H. and Maier-Reimer, E.: Using chemical tracers to assess ocean models, *Rev. Geophys.*, 39, 29–70, 2001.

**¹⁴C-age tracers in
global ocean
circulation models**

W. Koeve et al.

Title Page

Abstract

Introduction

Conclusions

References

Tables

Figures



Back

Close

Full Screen / Esc

Printer-friendly Version

Interactive Discussion



Feely, R. A., Sabine, C. L., Lee, K., Millero, F. J., Lamb, M. F., Greeley, D., Bullister, J. L., Key, R. M., Peng, T.-H., Kozyr, A., Ono, T., and Wong, C. S.: In situ calcium carbonate dissolution in the Pacific Ocean, *Global Biogeochem. Cy.*, 16, 1144, doi:10.1029/2002GB001866, 2002.

5 Fiaderio, M. E.: Three-dimensional modeling of tracers in the deep Pacific Ocean II. Radiocarbon and the circulation, *J. Mar. Res.*, 40, 537–550, 1982.

Follows, M. J., Ito, T., and Dutkiewicz, S.: On the solution of the carbonate chemistry system in the ocean biogeochemistry models, *Ocean Model.*, 12, 290–301, 2006.

10 Franke, J., Schulz, M., Paul, A., and Adkins, J. F.: Assessing the ability of the ¹⁴C projection-age method to constrain the circulation of the past in a 3-D ocean model, *Geochem. Geophys. Geosy.*, 9, Q08003, doi:10.1029/2008GC001943, 2008a.

Franke, J., Paul, A., and Schulz, M.: Modeling variations of marine reservoir ages during the last 45 000 years, *Clim. Past*, 4, 125–136, doi:10.5194/cp-4-125-2008, 2008b.

15 Ito, T., Follows, M. J., and Boyle, E. A.: Is AOU a good measure of respiration in the ocean?, *Geophys. Res. Lett.*, 31, L17305, doi:10.1029/2004GL020900, 2004.

Jain, A. K., Khesgi, H. S., Hoffert, M. I., and Wuebbles, D. J.: Distribution of radiocarbon as a test of global carbon cycle models, *Global Biogeochem. Cy.*, 9, 153–166, 1995.

Jenkins, W. J.: Oxygen utilization rates in North Atlantic subtropical gyre and primary production in oligotrophic systems, *Nature*, 300, 246–248, 1982.

20 Khatiwala, S.: A computational framework for simulation of biogeochemical tracers in the ocean, *Global Biogeochem. Cy.*, 21, GB3001, doi:10.1029/2007GB002923, 2007.

Khatiwala, S., Visbeck, M., and Schlosser, P.: Age tracers in an ocean GCM, *Deep-Sea Res. Pt. I*, 48, 1432–1441, 2001.

Khatiwala, S., Visbeck, M., and Cane, M. A.: Accelerated simulation of passive tracers in ocean circulation models, *Ocean Model.*, 9, 51–69, 2005.

25 Khatiwala, S., Primeau, F., and Holzer, M.: Ventilation of the deep ocean constrained with tracer observations and implications for radiocarbon estimates of ideal mean age, *Earth Planet. Sc. Lett.*, 325, 116–125, 2012.

30 Keller, D. P., Oschlies, A., and Eby, M.: A new marine ecosystem model for the University of Victoria Earth System Climate Model, *Geosci. Model Dev.*, 5, 1195–1220, doi:10.5194/gmd-5-1195-2012, 2012.

**¹⁴C-age tracers in
global ocean
circulation models**

W. Koeve et al.

Title Page

Abstract

Introduction

Conclusions

References

Tables

Figures



Back

Close

Full Screen / Esc

Printer-friendly Version

Interactive Discussion



- Koeve, W., Duteil, O., Oschlies, A., Kähler, P., and Segschneider, J.: Methods to evaluate CaCO_3 cycle modules in coupled global biogeochemical ocean models, *Geosci. Model Dev.*, 7, 2393–2408, doi:10.5194/gmd-7-2393-2014, 2014.
- Kriest, I., Khatiwala, S., and Oschlies, A.: Towards and assessment of simple global marine biogeochemical models of different complexity, *Prog. Oceanogr.*, 86, 337–360, 2010.
- Kriest, I., Oschlies, A., and Khatiwala, S.: Sensitivity analysis of simple global marine biogeochemical models, *Global Biogeochem. Cy.*, 26, GB2029, doi:10.1029/2011GB004072, 2012.
- Lynch-Stieglitz, J.: Tracers of past ocean circulation, in: *Treatise on Geochemistry*, 6, 433–451, 2003.
- Marshall, J. and Speer, K.: Closure of the meridional overturning circulation through Southern Ocean upwelling, *Nat. Geosci.*, 5, 171–180, doi:10.1038/NCEO1391, 2012.
- Marshall, J., Adcroft, A., Hill, C., Perelman, L., and Heisey, C.: A finite-volume, incompressible navier-stokes model for studies of the ocean on parallel computers, *J. Geophys. Res.*, 102, 5733–5752, 1997.
- Matsumoto, K.: Radiocarbon-based circulation age of the world ocean, *J. Geophys. Res.*, 112, C09004, doi:10.1029/2007JC004095, 2007.
- Matsumoto, K., Sarmiento, J. L., Key, R. M., Aumont, O., Bullister, J. L., Caldeira, K., Campin, J.-M., Doney, S. C., Drange, H., Dutay, J.-C., Follows, M., Gao, Y., Gnanadesikan, A., Gruber, N., Ishida, A., Joos, F., Lindsay, K., Maier-Reimer, E., Marshall, J. C., Matear, R. J., Monfray, P., Mouchet, A., Najjar, R., Plattner, G.-K., Schlitzer, R., Slater, R., Swathi, P. S., Totterdell, I. J., Weirig, M.-F., Yamanaka, Y., Yool, A., and Orr, J. C.: Evaluation of ocean carbon cycle models with data-based metrics, *Geophys. Res. Lett.*, 31, L07303, doi:10.1029/2003GL018970, 2004.
- Najjar, R. G., Jin, X., Louanchi, F., Aumont, O., Caldeira, K., Doney, C. S., Dutay, J.-C., Follows, M., Gruber, N., Joos, F., Lindsay, K., Maier-Reimer, E., Matear, R. J., Matsumoto, K., Monfray, P., Mouchet, A., Orr, J. C., Plattner, G.-K., Sarmiento, J. L., Schlitzer, R., Slater, R. D., Wierig, M.-F., Yamanaka, Y., and Yool, A.: Impact of circulation on export production, dissolved organic matter, and dissolved oxygen in the ocean: results from phase II of the Ocean Carbon-cycle Model Intercomparison Project (OCMIP-2), *Global Biogeochem. Cy.*, 21, GB3007, doi:10.1029/2006GB002857, 2007.
- Orr, J., Najjar, R., Sabine, C. L., and Joos, F.: Abiotic-HOWTO. Internal OCMIP Report, LSCE/CEA Saclay, Gif-sur-Yvette, France, 25 pp., available at: <http://ocmip5.ipsl.jussieu.fr/>

**¹⁴C-age tracers in
global ocean
circulation models**

W. Koeve et al.

Title Page

Abstract

Introduction

Conclusions

References

Tables

Figures



Back

Close

Full Screen / Esc

Printer-friendly Version

Interactive Discussion



OCMIP/phase2/simulations/Abiotic/HOWTO-Abiotic.html (last access: 28 November 2013), 1999.

Oschlies, A., Schulz, K. G., Riebesell, U., and Schmittner, A.: Simulated 21st century's increase in oceanic suboxia by CO₂-enhanced biotic carbon export, *Global Biogeochem. Cy.*, 22, GB4008, doi:10.1029/2007GB003147, 2008.

Rafter, T. A. and Fergusson, G. J.: Atom bomb effect – recent increase of carbon-14 content of the atmosphere and the biosphere, *Science*, 126, 557–558, 1957.

Redfield, A. C., Ketchum, B. H., and Richards, F. A.: The influence of organisms on the composition of seawater, in: *The Sea*, Vol. 2, edited by: Hill, M. N., John Wiley & Sons, New York, 26–77, 1963.

Rubin, S. I. and Key, R. M.: Separating natural and bomb-produced radiocarbon in the ocean: the potential alkalinity method, *Global Biogeochem. Cy.*, 16, 1105, doi:10.1029/2001GB001432, 2002.

Sarmiento, J. L., Thiele, G., Key, R. M., and Moore, W. S.: Oxygen and nitrate new production and remineralization in the North Atlantic subtropical gyre, *J. Geophys. Res.*, 95, 18303–18315, 1990.

Schmittner, A., Oschlies, A., Matthews, H. D., and Galbraith, E. D.: Future changes in climate, ocean circulation, ecosystems, and biogeochemical cycling simulated for a business-as-usual CO₂ emission scenario until year 4000 AD, *Global Biogeochem. Cy.*, 22, GB1013, doi:10.1029/2007GB002953, 2008.

Stammer, D., Ueyoshi, K., Köhl, A., Large, W. G., Josey, S. A., and Wunsch, C.: Estimating air–sea fluxes of heat, freshwater, and momentum through global ocean data assimilation, *J. Geophys. Res.*, 109, C05023, doi:10.1029/2003JC002082, 2004.

Stuiver, M.: ¹⁴C distribution in the Atlantic Ocean, *J. Geophys. Res.*, 85c, 2711–2718, 1980.

Stuiver, M. and Polach, H. A.: Reporting of ¹⁴C data, *Radiocarbon*, 19, 355–363, 1977.

Stuiver, M., Quay, P. D., and Ostlund, H. G.: Abyssal water carbon-14 distribution and the age of the world ocean, *Science*, 219, 849–851, 1983.

Suess, H.: Radiocarbon concentration in modern wood, *Science*, 122, 415–417, 1955.

Sweeney, C., Gloor, E., Jacobson, A. R., Key, R. M., McKinley, G., Sarmiento, J. L., and Wanninkhof, R.: Constraining global air–sea gas exchange for CO₂ with recent bomb ¹⁴C measurements, *Global Biogeochem. Cy.*, 21, GB2015, doi:10.1029/2006GB002784, 2007.

Thiele, G. and Sarmiento, J. L.: Tracer dating and ocean ventilation, *J. Geophys. Res.*, 95, 9377–9391, 1990.

Toggweiler, J. R., Dixon, K., and Bryan, K.: Simulations of radiocarbon in a coarse-resolution world ocean model. 1. steady state prebomb distribution, *J. Geophys. Res.*, 94, 8217–8242, 1989.

Trenberth, K. E., Large, W. G., and Olson, J. G.: A Global Ocean Wind Stress Climatology Based on ECMWF Analyses, National Center for Atmospheric Research, 93 pp., 1989.

Weaver, A. J., Eby, M., Wiebe, E. C., Bitz, C. M., Duffy, P. B., Ewen, T. L., Fanning, A. F., Holland, M. M., MacFadyen, A., Matthews, H. D., Meissner, K. J., Saenko, O., Schmittner, A., Wang, H., and Yoshimori, M.: The UVIC earth system climate model: model description, climatology, and applications to past, present and future climates, *Atmos. Oceans*, 39, 361–428, 2001.

GMDD

7, 7033–7074, 2014

¹⁴C-age tracers in global ocean circulation models

W. Koeve et al.

Title Page

Abstract

Introduction

Conclusions

References

Tables

Figures



Back

Close

Full Screen / Esc

Printer-friendly Version

Interactive Discussion



**¹⁴C-age tracers in
global ocean
circulation models**

W. Koeve et al.

[Title Page](#)[Abstract](#)[Introduction](#)[Conclusions](#)[References](#)[Tables](#)[Figures](#)[◀](#)[▶](#)[◀](#)[▶](#)[Back](#)[Close](#)[Full Screen / Esc](#)[Printer-friendly Version](#)[Interactive Discussion](#)**Table 1.** Tracers.

component	¹⁴ C-based tracers: are subject to non-linear tracer mixing effect name of tracer (name of age)	ideally behaving tracers: are NOT subject to non-linear tracer mixing effect name of tracer = name of age
preformed circulation	¹⁴ C-DIC ^{pre} (¹⁴ C-age ^{pre}) ¹⁴ C-DIC ^{decay} (¹⁴ C-age ^{decay})	age ^{pre} age ^{ideal}
total	¹⁴ C-DIC ^{bulk} (¹⁴ C-age ^{bulk})	age ^{bulk}

^{14}C -age tracers in global ocean circulation models

W. Koeve et al.

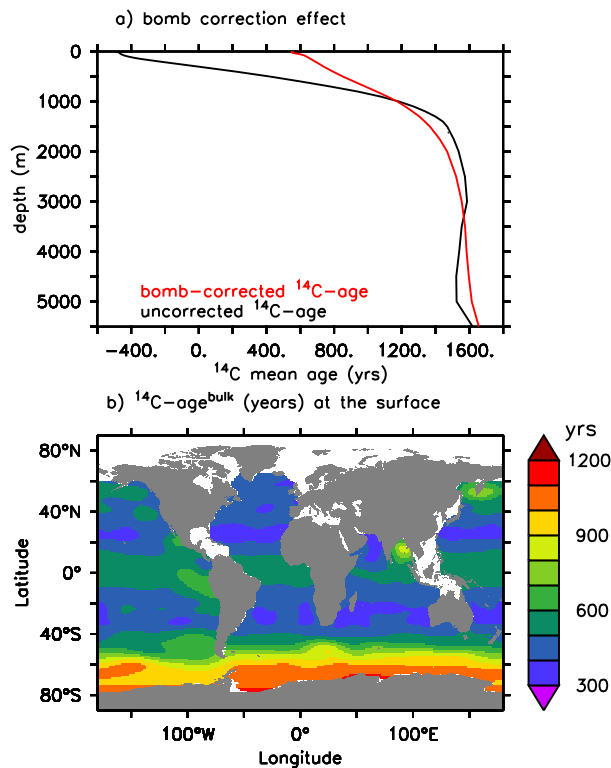


Figure 1. (a) Global mean profiles (GLODAP) of bulk ^{14}C -age (red) and the pseudo age of ^{14}C -DIC not corrected for the effects of bomb and anthropogenic ^{14}C signatures. (b) Map of bulk ^{14}C -age at the surface of the Ocean (GLODAP).

^{14}C -age tracers in global ocean circulation models

W. Koeve et al.

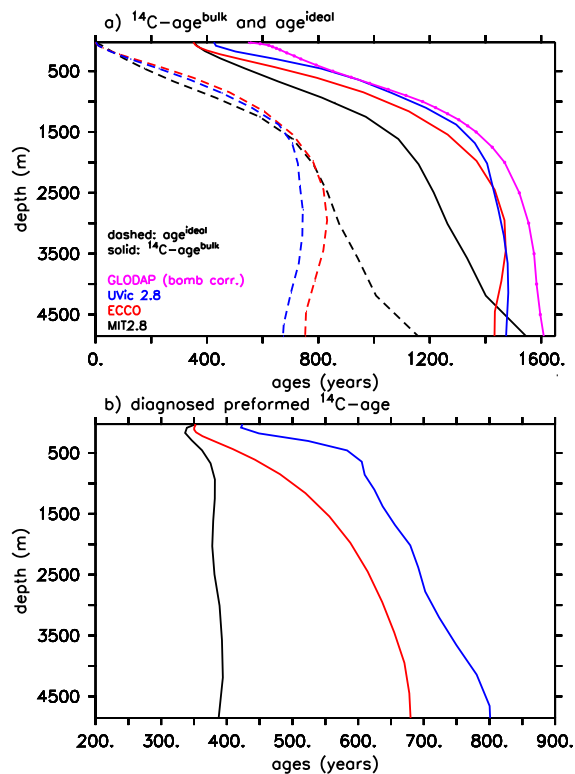


Figure 2. (a) Global mean profiles of bulk ^{14}C -age (solid lines) and ideal age (dashed lines) for three different global ocean circulation models (color code see figure insert) and the GLODAP database (solid magenta). (b) Global mean profiles of the difference between bulk ^{14}C -age and ideal age for three different global ocean circulation models (colour code as a).

**¹⁴C-age tracers in
global ocean
circulation models**

W. Koeve et al.

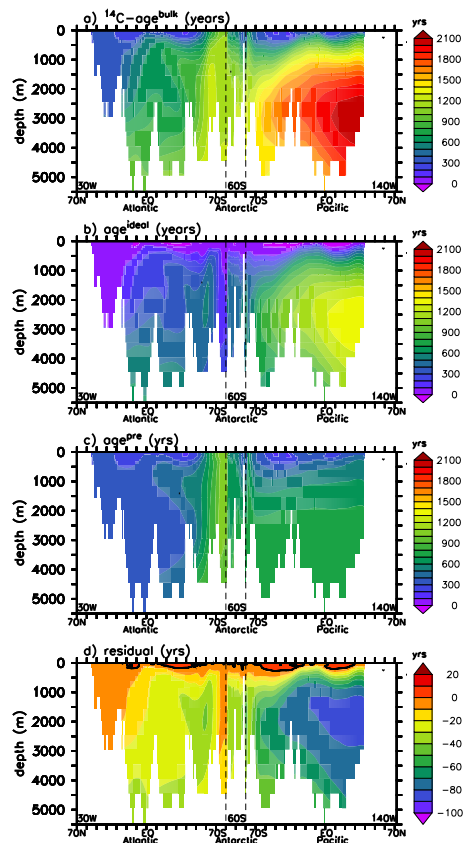


Figure 3. Bulk ^{14}C -age (a), ideal age (b) and preformed age (c) from the ECCO experiment along a combined section through the North Atlantic (30°W), the Southern Ocean (60°S), and the Pacific Ocean (140°W). The preformed age is taken from the age^{pre} tracer (see Sect. 2.2 for tracer definition). (d) shows the residual ($^{14}\text{C}\text{-age}^{\text{bulk}} - \text{age}^{\text{ideal}} - \text{age}^{\text{pre}}$), i.e. the third term on the right hand side of Eq. (4).

Title Page

Abstract

Introduction

Conclusions

References

Tables

Figures



Back

Close

Full Screen / Esc

Printer-friendly Version

Interactive Discussion



^{14}C -age tracers in global ocean circulation models

W. Koeve et al.

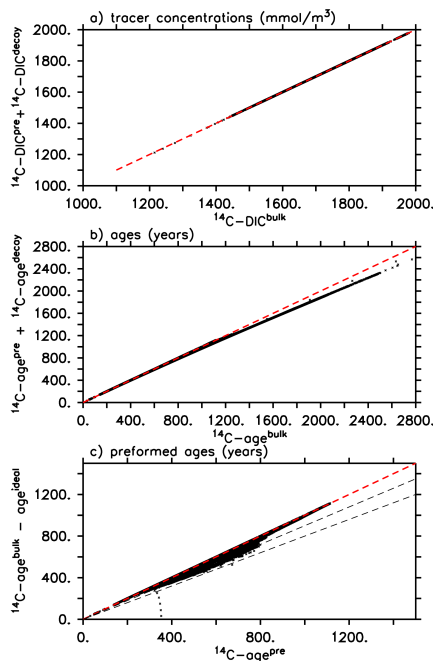


Figure 4. Scatter plots **(a)** of ^{14}C -DIC tracer concentrations vs. the sum of ^{14}C -DIC^{pre} and ^{14}C -DIC^{decay} tracer concentrations and **(b)** bulk ^{14}C -age vs. the sum of ages computed from ^{14}C -DIC preformed and decay tracers. Note that a few grid cells with ^{14}C -DIC concentrations below about 1300 mmol m^{-3} and bulk ages above about 2600 yr are not fully in steady state after the 2500 yr run time of this model experiment. We ignore these grid cells in the discussion. **(c)** Comparison of ages derived from the ^{14}C -DIC preformed tracer and by difference of the bulk ^{14}C -DIC tracer and the ideal age tracer. Red dashed line is the 1 : 1 line, dashed grey lines indicate -10 and -20% isolines.

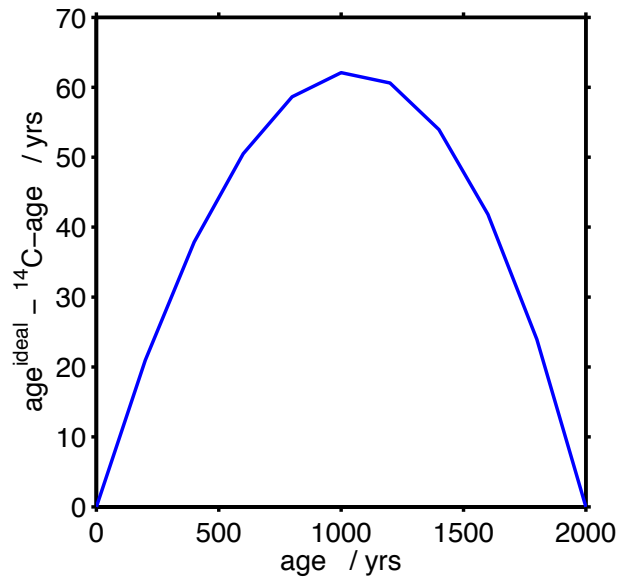


Figure 5. Simple 2-endmember mixing-model prediction of the low-bias of ¹⁴C-based ages compared to ideal age tracers (for details see text).

¹⁴C-age tracers in global ocean circulation models

W. Koeve et al.

Title Page

Abstract Introduction

Conclusions References

Tables Figures

◀ ▶

◀ ▶

Back Close

Full Screen / Esc

Printer-friendly Version

Interactive Discussion



^{14}C -age tracers in global ocean circulation models

W. Koeve et al.

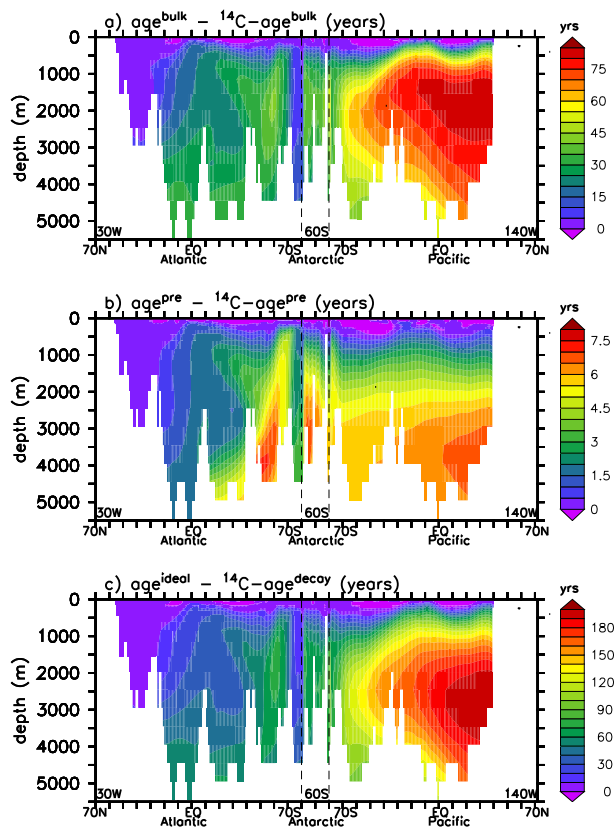


Figure 6. Anomalies (ideally behaving tracer – ^{14}C -based tracer) of bulk age (a), preformed component of age (b) and circulation component of age (c).

Title Page

Abstract

Introduction

Conclusions

References

Tables

Figures



Back

Close

Full Screen / Esc

Printer-friendly Version

Interactive Discussion



¹⁴C-age tracers in global ocean circulation models

W. Koeve et al.

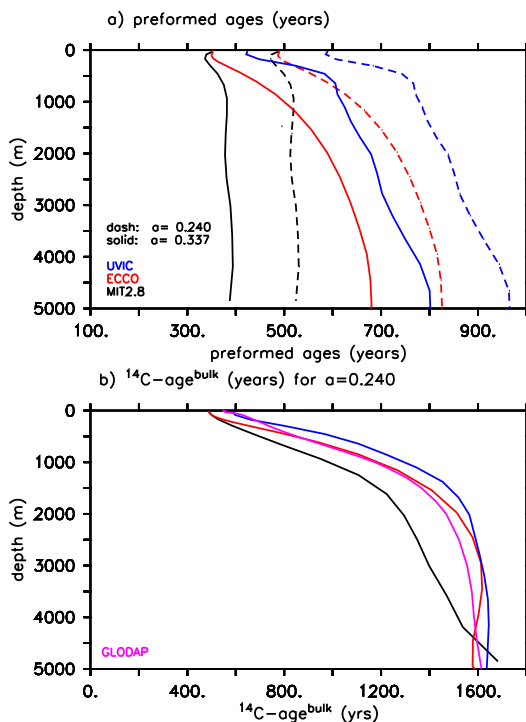


Figure 8. Sensitivity of preformed and bulk ¹⁴C-age to the choice of the gas exchange parameter a of Eq. (1). **(a)** preformed ¹⁴C-age for $a = 0.337$ (solid lines) and $a = 0.24$ (dashed lines). Results from MIT2.8 (black), ECCO (red), and UVIC (blue) are shown. **(b)** Global mean profiles of ¹⁴C-age^{bulk} using $a = 0.24$.

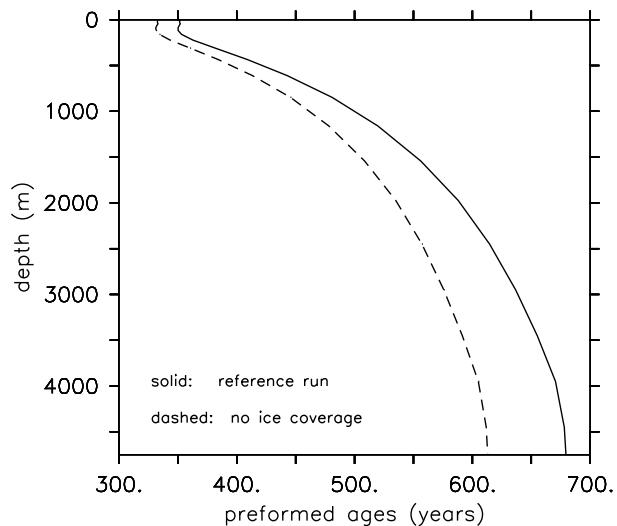


Figure 9. Sensitivity of preformed ^{14}C -age to ice cover. Solid line: control with ice cover affecting CO_2 gas exchange, dashed: effect of ice cover on CO_2 gas exchange ignored. Results are from the ECCO model, both runs use identical circulation.

^{14}C -age tracers in global ocean circulation models

W. Koeve et al.

Title Page

Abstract Introduction

Conclusions References

Tables Figures

◀ ▶

◀ ▶

Back Close

Full Screen / Esc

Printer-friendly Version

Interactive Discussion



¹⁴C-age tracers in global ocean circulation models

W. Koeve et al.

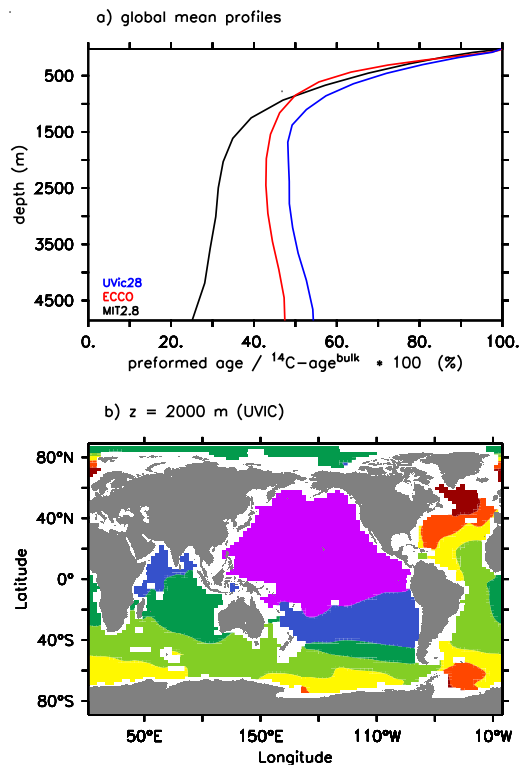


Figure 10. (a) Global mean profiles of the relative contribution (%) of preformed age (estimated as bulk ^{14}C -age – ideal age) to the bulk ^{14}C -age. (b) As Fig. 10a, but for the UVIC model in 2000 m depths, displaying that even in the oldest waters of the North Pacific the preformed age is a significant component of the bulk age.

Title Page

Abstract

Introduction

Conclusions

References

Tables

Figures



Back

Close

Full Screen / Esc

Printer-friendly Version

Interactive Discussion



¹⁴C-age tracers in global ocean circulation models

W. Koeve et al.

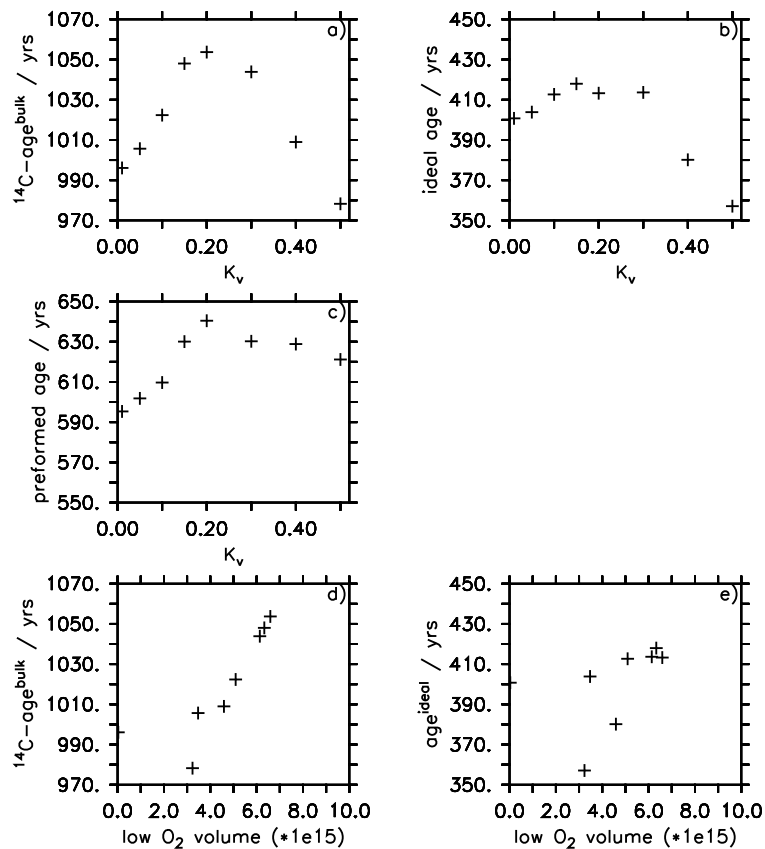


Figure 11. Sensitivity of ages of suboxic waters to vertical diffusivity (K_v) in the UVIC model. **(a)** Bulk age, **(b)** ideal age, **(c)** preformed age. Scatterplots of bulk age **(d)** and ideal age **(e)** vs. volume of suboxic waters in the model runs.

^{14}C -age tracers in global ocean circulation models

W. Koeve et al.

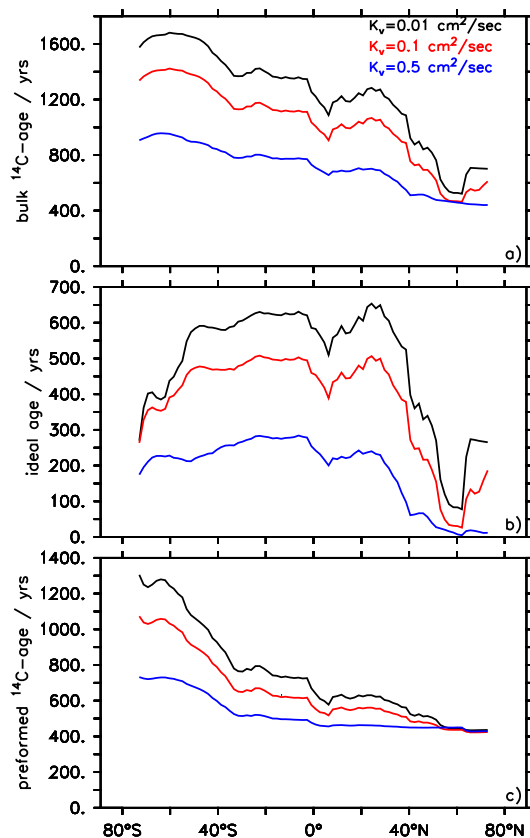


Figure 12. Sensitivity of Atlantic Ocean age patterns to vertical diffusivity (K_v) in the UVIC model. **(a)** Bulk ^{14}C -age, **(b)** ideal age, **(c)** preformed ^{14}C -age. Preformed ^{14}C -age is diagnosed here from the difference of bulk age and ideal age.

Title Page

Abstract

Introduction

Conclusions

References

Tables

Figures

◀

▶

◀

▶

Back

Close

Full Screen / Esc

Printer-friendly Version

Interactive Discussion



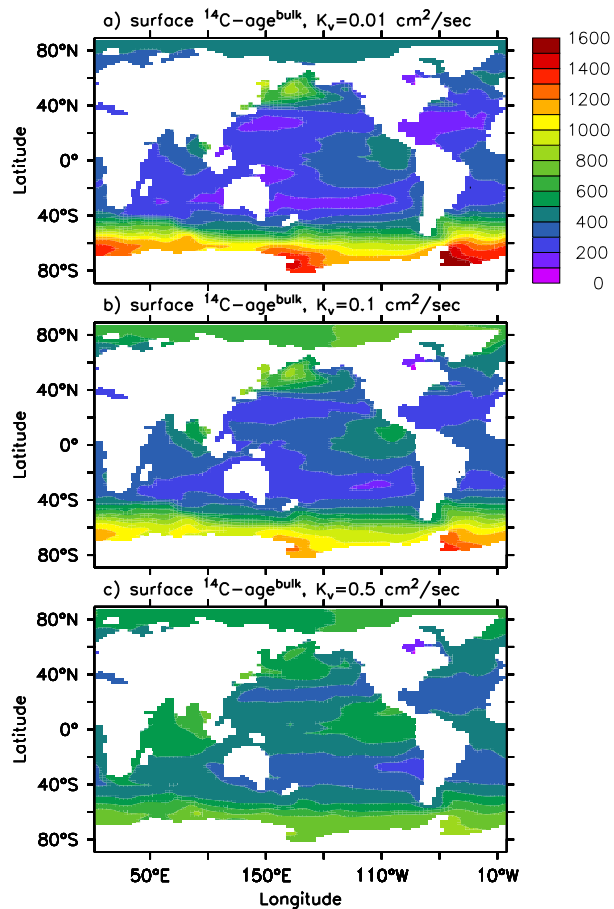


Figure 13. Surface bulk ^{14}C -age in the UVIC model for three different K_v values. **(a)** $K_v = 0.01 \text{ cm}^2 \text{ s}^{-1}$, **(b)** $K_v = 0.1 \text{ cm}^2 \text{ s}^{-1}$ and **(c)** $K_v = 0.5 \text{ cm}^2 \text{ s}^{-1}$.

Title Page

Abstract

Introduction

Conclusions

References

Tables

Figures



Back

Close

Full Screen / Esc

Printer-friendly Version

Interactive Discussion



**^{14}C -age tracers in
global ocean
circulation models**

W. Koeve et al.

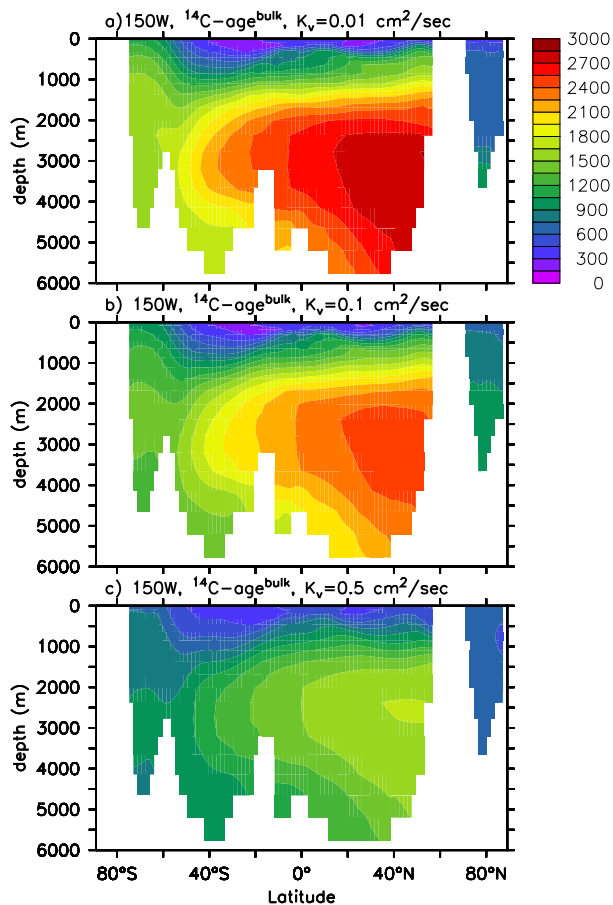


Figure 14. Vertical section along 150° W of bulk ^{14}C -age in the UVIC model for three different K_v values. **(a)** $K_v = 0.01$ cm² s⁻¹, **(b)** $K_v = 0.1$ cm² s⁻¹ and **(c)** $K_v = 0.5$ cm² s⁻¹.

Title Page

Abstract

Introduction

Conclusions

References

Tables

Figures

◀

▶

◀

▶

Back

Close

Full Screen / Esc

Printer-friendly Version

Interactive Discussion

